

DFT study of the pressure influence on the electronic and magnetic properties of $\text{Ga}_x\text{Mn}_{1-x}\text{N}$ compound

Miguel J. Espitia R., Octavio Salcedo Parra, and John H. Díaz F.

GEFEM Group, Distrital University Francisco José de Caldas, Bogotá Colombia,

e-mail: mespitiar@udistrital.edu.co; ojsalcedop@udistrital.edu.co; jhdiazf@udistrital.edu.co

Received 1 April 2013; accepted 2 May 2013

We report a first-principles study of the pressure dependence of electronic and the magnetic properties of $\text{Ga}_x\text{Mn}_{1-x}\text{N}$ compounds ($x = 0.25, 0.50$ and 0.75) in wurtzite-derived structures. We use the full-potential linearized augmented plane wave method (FP-LAPW) within of the density functional theory framework. We found that, the lattice constant vary linearly with Ga-concentration. The magnetic moment changes for a critical pressure. At $x = 0.75$, a rather abrupt onset of the magnetic moment from 0 to $6.02 \mu_B$ at $P_{cr} = 26.50$ GPa is observed. For $x = 0.25$ and 0.50 Ga concentrations, the magnetic moment increases gradually when the pressure decreases toward the equilibrium value. We study the transition pressure dependence to a ferromagnetic phase near the onset of magnetic moment for each $\text{Ga}_x\text{Mn}_{1-x}\text{N}$ compounds. The calculation of the density of states with Ga concentration is carried out considering two spin polarizations. The results reveal that for $x = 0.75$ the compound behaves as a conductor for the spin-up polarization and that the density of states for spin-down polarization is zero at the Fermi level. At this concentration the compound presents a half metallic behavior; therefore this material could be potentially useful as spin injector. At high pressures $P > P_{cr}$ the compounds exhibit a metallic behavior.

Keywords: FP-LAPW; magnetic semiconductors; pressure dependence.

PACS: 68.35.B; 68.35.Md; 68.43.Bc; 68.43.Fg

1. Introduction

At present time, various high performance devices fabricated from III-nitride have generated great interest. Amongst the III semiconductor, Gallium nitride (GaN), whose more stable phase is hexagonal (wurtzite) [1]. Due to its wide direct band gap, gallium nitride is a promising candidate in semiconductor technology and has a broad range of potential applications for optoelectronic and high power electronic devices. Intensive activities over the recent years have made of the short wave length blue, violet light emitting diodes (LEDs) a commercial reality [2]. Due to its high chemical stability and high thermal conductivity, is also suitable for the applications in the harsh environments, such as, in high-temperature/high-power electronic devices [3,4], as metal-semiconductor field effect transistors (MESFETs), high electron mobility transistors (HEMTs) and heterojunction bipolar transistors (HBTs) [5,6]. Large piezoelectric constants of GaN point out possible applications of GaN-based materials in piezoelectric sensors [1]. Additionally, theoretically [7,8] and experimentally [9], high Curie temperatures and room-temperature ferromagnetism have been found in GaN-doped with transition-metal (MT) elements, which in principle opens the door for potentials use of this room-temperature ferromagnetic material for spintronic devices [7-10]. The magnetic properties of transition metal (MT) in GaN regained prominence due to potential application for Dilute Magnetic Semiconductors (DMS) [11,12]. In particular, the 3d-MT elements can be expected that substitute Ga-atoms during crystal growth. The knowledge of their associated deep defects is very important to development a new kind of devices such as: electro-optic switches, ultra sen-

sitive magnetic field sensors and quantum-mechanism-based logic for high speed computation [13]. In this paper, we investigate mixed $\text{Ga}_x\text{Mn}_{1-x}\text{N}$ compounds. As will be shown, the dilution of MnN with Ga expands the lattice constant according to Vegard's law as expected. Also Ga incorporation produce the arise of magnetic moment formation. This makes these materials potentially useful as spin injector. In order to model the compounds, simple ordered model structures ($\text{Ga}_1\text{Mn}_3\text{N}_4$, $\text{Ga}_1\text{Mn}_1\text{N}_2$, $\text{Ga}_3\text{Mn}_1\text{N}_4$) based on supercells of the wurtzite structure were investigated.

2. Computational method

The electronic structure calculations were performed employing the full-potential linearized augmented plane wave method (FP-LAPW) as implemented in the WIEN2k package, which includes the LAPW [14], within of the spin density functional theory (DFT) framework [15,16]. The exchange and correlations electronic energy were calculated with Generalized Gradient Approximation (GGA) of Perdew *et al.* [17]. The method FP-LAPW the cell is divided into two regions, the atomic spheres centered on the nuclei and the interstitial region nonoverlapping. Inside the atomic spheres the wave functions are replaced by atomic functions, whereas that in interstitial region, the function is expanded in plane waves. Separation energy between the valence and core states of -8.0 Ry, and the angular momenta up to $l_{max} = 10$, were used. The wave functions in the interstitial region were expanded in plane waves with a cutoff of $K_{max} = 8.0/RMT$ (where RMT is the smallest muffin-tin sphere radii inside the cell). For $\text{Ga}_x\text{Mn}_{1-x}\text{N}$ compounds muffin-tin radii of 1.90, 1.80 and 1.60 bohr for Ga, Mn and N atoms were selected

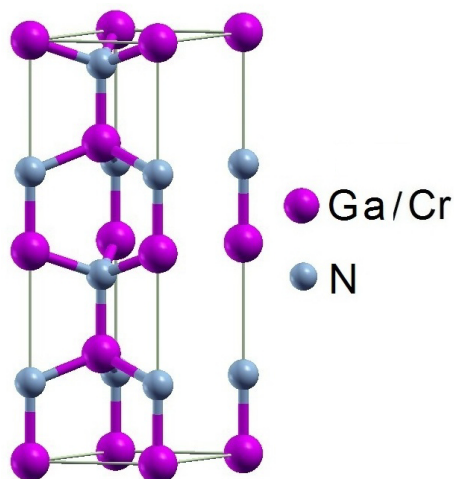


FIGURE 1. Unit cell used in our calculation for $\text{Ga}_x\text{Mn}_{1-x}\text{N}$ compounds in wurtzite-like structure.

respectively. In calculation of the electronic structure, a 144 k-points mesh were used in Brillouin irreducible zone generated according to the Monkhorst Pack scheme [18]. The iteration for self-consistency was continued until the convergence criterium of 1×10^{-4} Ry was reached.

The $\text{Ga}_x\text{Mn}_{1-x}\text{N}$ compounds were modeled for $x=0.25$, 0.50 and 0.75 compositions according to special quasirandom structures approach [19] and the disorder aspects were ignored. For $\text{Ga}_1\text{Mn}_1\text{N}_2$ ($x=0.50$) an hexagonal unit cell with alternating [0001] layers of MnN and GaN in conventional wurtzite structure was employed. For $\text{Ga}_1\text{Mn}_3\text{N}_4$ ($x = 0.25$) and $\text{Ga}_3\text{Mn}_1\text{N}_4$ ($x = 0.75$) an hexagonal unit cell consisting of two wurtzite unit cells piled in the c direction were used [20]. There are eight planes with one Ga (or Mn) or one N atom in a 1×1 configuration, as shown in Fig. 1. In this structure, a Mn atom replaces to a Ga atom in the unit cell. This atomic substitution (Mn-Ga) has been experimentally observed; R. Vidyasagar *et al.* [21] for Mn doped GaN successfully grown on sapphire (0001) substrate using plasma assisted Molecular Beam Epitaxy. Also Zdenek Sofer *et al.* [22] used metalorganic vapor-phase epitaxy (MOVPE) technique, successfully grown of $\text{Ga}_{1-x}\text{Mn}_x\text{N}$; additionally, C. X. Gao *et al.* [23] Mn-doped GaN films grown on sapphire by using a single GaN precursor via molecular beam epitaxy. This has allowed to get room temperature ferromagnetism of Mn-doped GaN single crystals has stirred further interest in the DMS systems [23,24]. The lattice parameters and cohesion energy were found by the fitting the total energy versus volume to the Murnaghan's state equation [25].

3. Results and discussion

The cohesion energy per unit cell as function of lattice constant for $\text{Ga}_x\text{Mn}_{1-x}\text{N}$ compounds are shown in Fig. 2. As we showing figure, the minimum for each curve shifts to the right as it increases the concentration of Ga in the $\text{Ga}_x\text{Mn}_{1-x}\text{N}$ compound.

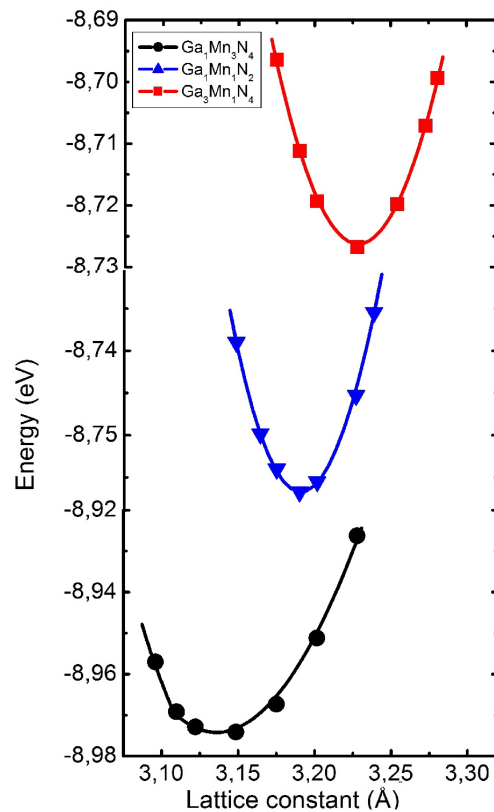


FIGURE 2. Cohesion energy as a function of the lattice constant for $\text{Ga}_x\text{Mn}_{1-x}\text{N}$ compound, the line is a Murnaghan equation of state fit.

From minimum point energy of Fig. 2, the equilibrium lattice constant (square points blue) and the energy (circular points red) per unit cell as a function of Ga concentration are presented in Fig. 3. The increase of lattice constant with Ga concentration is due to that Ga-atom is bigger than Mn-atom. We found a linear dependence according to Vegard's law. Note that the energy also has a linear tendency with the Ga concentration as has been observed in other ternary nitrides [20,26].

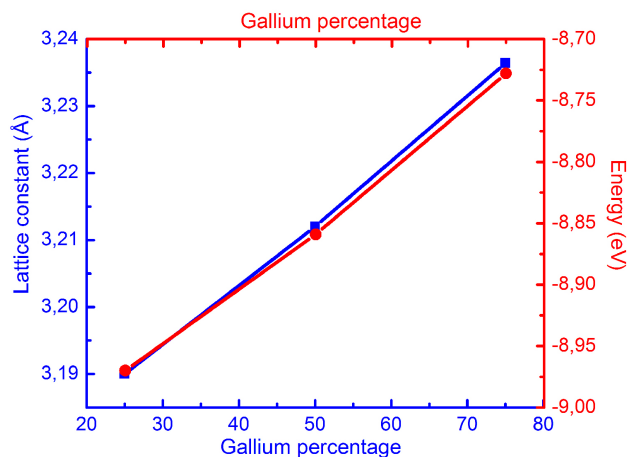


FIGURE 3. Equilibrium lattice constant and cohesion energy as function of Ga concentration in $\text{Ga}_x\text{Mn}_{1-x}\text{N}$

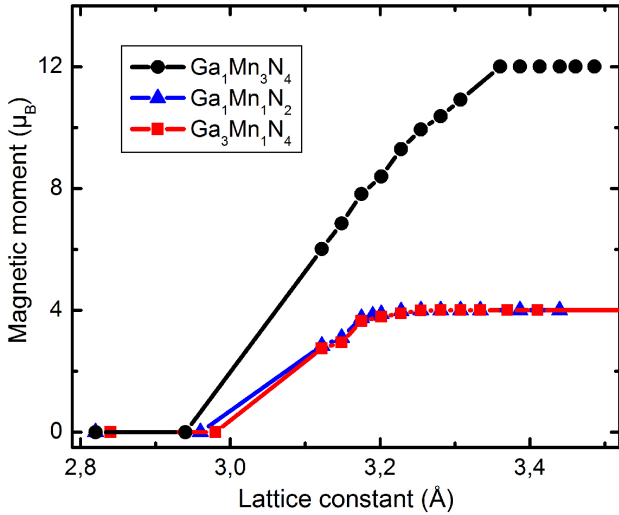


FIGURE 4. Magnetic moment per unit/cell as a function of the lattice constant for $\text{Ga}_x\text{Mn}_{1-x}\text{N}$. The line is guide to the eye.

Magnetic moment for $\text{Ga}_x\text{Mn}_{1-x}\text{N}$ compounds are shown in Fig. 4. As we shown in this figure, for $\text{Ga}_1\text{Mn}_3\text{N}_4$ (circular points) there is a rather abrupt onset of the magnetic moment from 0 to $6.02 \mu\text{B}$ at $\sim 26.50 \text{ GPa}$ (3.12 \AA). The $\text{Ga}_1\text{Mn}_1\text{N}_2$ and $\text{Ga}_3\text{Mn}_1\text{N}_4$ compounds presented the same magnetic moment but with a slowly pressure dependence. From this figure, we observe the tendency towards magnetic moment increases as we further decrease the pressure. A similar behavior has been reported by González *et al.* [27] $\text{Ga}_x\text{V}_{1-x}\text{N}$ compounds in wurtzita structures

We found that in the studied cases, $\text{Ga}_x\text{Mn}_{1-x}\text{N}$ has a nonzero magnetic moment at the zero pressure. Comparing the total energy of the ferromagnetic (FM) and anti-ferromagnetic (AFM) configurations for $x = 0.25$ and 0.50 compounds at the equilibrium volume, the FM is found to be lower in energy and is the predicted to be preferred state. Such as has been found experimentally Biswas Kanishka *et al.* [28] and Sang Eon Park *et al.* [29] for diluted concentrations of Mn atoms in the GaN semiconductor. In Table I we show a summary of the structural and magnetic results for $\text{Ga}_x\text{Mn}_{1-x}\text{N}$ compounds. We give the equilibrium lattice constant (a_0), critical pressure at which the magnetic moment appears (P_{cr}), saturation value of the magnetic moment per unit cell (μ) and the spin polarization P_F at the equilibrium lattice constant defined by:

$$P_F = \frac{N_{\uparrow}(E_F) - N_{\downarrow}(E_F)}{N_{\uparrow}(E_F) + N_{\downarrow}(E_F)}$$

With $N_S(E_F)$ being the DOS of spin S ($=$ up or down) for the Fermi energy E_F . In Table I, we note that the calculated magnetic moment for each configuration ($4 \mu\text{B}/\text{Mn-atom}$) is due to the Mn^{3+} electronic configuration (dominate the origin of room temperature ferromagnetism), because a Mn-atom provides two net electrons to the $\text{Ga}_x\text{Mn}_{1-x}\text{N}$ compound and the Mn atoms couple ferromagnetically when doped into GaN [30].

We study the pressure dependence on the electronic density of states (DOS) for the spin-up and spin-down polarization in $\text{Ga}_x\text{Mn}_{1-x}\text{N}$ compounds. In Fig. 5, we show the partial (PDOS) of d states of Manganese calculated per atom, and the total DOS estimated per unit cell of the $\text{Ga}_3\text{Mn}_1\text{N}_4$ compound at the equilibrium lattice constant ($P = 0$).

TABLE I. Structural and magnetic properties of $\text{Ga}_x\text{Mn}_{1-x}\text{N}$ compounds.

Compound	a_0 (Å)	P_{cr} (GPa)	P_F (%)
$\text{Ga}_3\text{Mn}_1\text{N}_4$	3,235	22,50	100
$\text{Ga}_1\text{Mn}_1\text{N}_2$	3,210	24,45	78,8
$\text{Ga}_1\text{Mn}_3\text{N}_4$	3,190	26,50	31,8

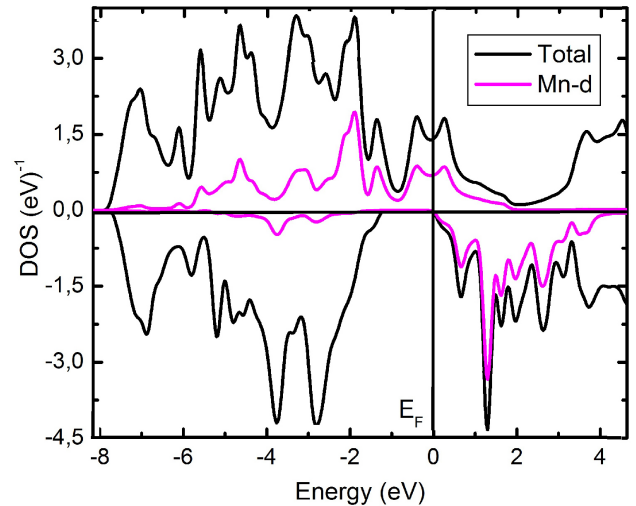


FIGURE 5. Partial DOS of d-states of manganese calculated per atom and total DOS estimated per unit cell of the $\text{Ga}_3\text{Mn}_1\text{N}_4$ compound at equilibrium pressure $P = 0$.

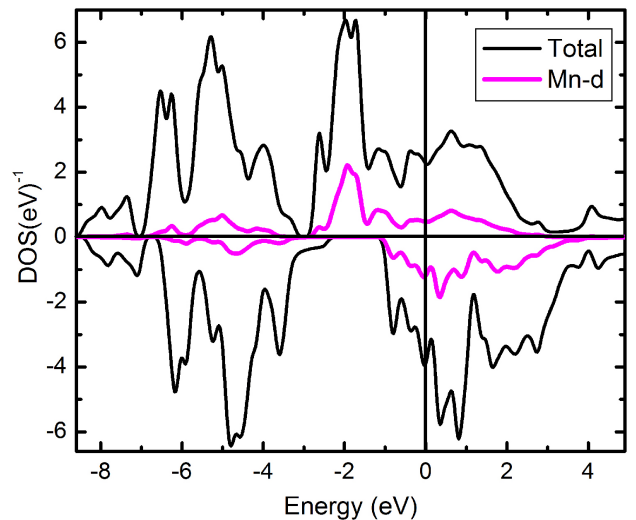


FIGURE 6. Partial DOS of d-states of manganese calculated per atom and total DOS estimated per unit cell of the $\text{Ga}_3\text{Mn}_1\text{N}_4$ compound at over the transition pressure $P > P_{cr}$ ($P = 34 \text{ GPa}$). Energy is relative to Fermi energy.

Near the Fermi level, the dispersion in the manganese impurity bands show that there is considerable interaction between neighboring Mn atoms in the unit cell. This compound behaves as conductor for spin-up polarization and as semiconductor for spin-down polarization. We found 100% spin polarization at the Fermi level which indicates that $\text{Ga}_3\text{Mn}_1\text{N}_4$ compound presents a half metallic behavior at $P = 0$. The Fig. 6 shows the density of states calculated at the high pressure $P = 34$ GPa over to the transition pressure $P > P_{cr}$. The Fermi level passes through the impurity and conduction bands in both spin polarization. The compound exhibits a metallic behavior. We can observe that the spin polarization splitting is dependent on the pressure and may be manipulated experimentally. Similar results we found for the other concentrations $\text{Ga}_1\text{Mn}_1\text{N}_2$ and $\text{Ga}_1\text{Mn}_3\text{N}_4$. On the basis of our present study, we believe that $\text{Ga}_x\text{Mn}_{1-x}\text{N}$ compounds may be candidates for being ferromagnetic or half-metallic materials in semiconductor-based spintronic applications.

4. Conclusions

A first-principles study of pressure effects on the electronic and magnetic properties of $\text{Ga}_x\text{Mn}_{1-x}\text{N}$ compounds ($x = 0.25, 0.50$ and 0.75) in wurtzite derived structures were presented. We used the full-potential linearized augmented plane wave LAPW within of the spin density functional the-

ory framework. The lattice constant is found to vary linearly with Ga-concentration. The magnetic moment changes for a critical pressure. At $x = 0.75$, a rather abrupt onset of the magnetic moment from to $6.02 \mu_B$ at ~ 26.50 GPa, is observed. For $x = 0.25$ and 0.50 Ga concentrations the magnetic moment increased gradually when pressure is decreased toward the equilibrium volume. Also, we study the pressure dependence of transition to a ferromagnetic phase near the onset of magnetic moment for each $\text{Ga}_x\text{Mn}_{1-x}\text{N}$ compounds. Calculation of the density of states with Ga concentration was carried out considering two spin polarizations. Results reveal that when $x = 0.75$ the compound behaves as conductor for spin-up polarization and as semiconductor for spin-down polarization is zero at the Fermi level. At this concentration compound has a possible half metallic behavior; therefore this material could be potentially useful as spin injector. At high pressures $P > P_{cr}$ the compounds exhibit a metallic behavior.

Acknowledgments

We want to thank to Research Center of the Distrital University CUID for financial support.

-
1. O. Arbouche, B. Belgoumene, B. Soudini and M. Driz, *Computational Materials Science*. **47** (2009) 432-438.
 2. S. Nakamura, *Solid State Communications*. **102** (1997) 237-243.
 3. S. Nakamura, M. Senoh, N. Iwasa and S.-i. Nagahama, *Applied Physics Letters*. **67** (1995) 1868.
 4. H. Bar-Ilan, S. Zamir, O. Katz, B. Meyler, J. Salzman, *Materials Science and Engineering A*. **302** (2001) 14-17
 5. R. J. Trew, M.W. Shin and V. Gatto, *Solid-State Electronics*. **41** (1997) 1561- 1567.
 6. S. J. Pearton, F. Ren, A.P. Zhang and K.P. Lee, *Materials Science and Engineering: R: Reports*. **30** (2000) 55-212.
 7. T. Dietl, H. Ohno, F. Matsukura, J. Cibert and D. Ferrand, *Science*. **287** (2000) 1019-1022.
 8. X. M. Cai, A. B. Djuricic, M .H. Xie, H. Liu, X. X. Zhang, J. J. Zhu and H. Yang, *Materials Science and Engineering B*. **117** (2005) 292-295.
 9. Joongoo Kang, K.J. Chang, *Physica B*. **376** (2006) 635-638.
 10. Yanlu Li, Weiliu Fan, Honggang Sun, Xiufeng Cheng, PanLi, Xian Zhao and Minhua Jiang, *Journal of Solid State Chemistry*. **183** (2010) 2662-2668.
 11. K. Sato, P.H. Dederics and H. Katayama-Yoshida, *Europhysics Letters*. **61** (2003) 403-408.
 12. S. J. Pearton *et al.*, *Thin Solid Films*. **447** (2004) 493-501.
 13. M. Souissi, A. Bchetnia and B. El Jani, *Journal of Crystal Growth*. **277** (2005) 57-63.
 14. Schwarz Karlheins. DFT calculations of solids with LAPW and WIEN2k. *Journal of Solid State Chemistry*. **176** (2003) 319-328.
 15. P. Blaha, K. Schwarz, G. Madsen, D. Kvasnicka and J. Luitz. WIEN2k, *An Augmented Plane Wave Plus Local Orbitals Program for Calculating Crystal Properties* (Vienna University of Technology) 2009. ISBN 3-9501031-1-2
 16. P. Hohenberg and W. Kohn, *Physical Review* **136** (1964) 864-871.
 17. P. Hohenberg and W. Kohn, *Physical Review* **136** (1964) 864-871.
 18. J. P. Perdew, K. Burke and M. Ernzerhof, *Physical Review Letters* **77** (1996) 3865-3868.
 19. H. J. Monkhorst and J.D. Pack, *Physical Review*, **13** (1976) 5188-5192.
 20. M. G. Moreno-Armenta, L. Mancera, N. Takeuchi, *Physica Status Solidi (b)*. **238** (2003) 127-135.
 21. R. Vidyasagar, Y. T. Lin and L. W. Tu. *Material Research Bulletin* **47** (2012) 4467-4471.
 22. Zdenek Sofer *et al.*, *journal of Crystal Growth* **310** (2008) 5025-5027.

23. C. X. Gao, F. C. Yu, D. J. Kim, H. J. Kim and Y. E. Ihm, *Journal of the Korean Physical Society*. **54** (2009) 633-636
24. I. T. Yoon, M.H. Ham, J.M. Myoung, *Applied Surface Science* **255** (2009) 4840-4843
25. F. D. Murnaghan, *Proceedings of the National Academy Science*. **30** (1944) 244-250.
26. P. William Lopez, M.G. Jairo Arbey Rodriguez and M.-Armenta, *Physica B: Condensed matter*. **398** (2007) 385-388.
27. R. Gonzalez Hernandez, W. Lopez Perez, F. Fajardo and J. Arbey Rodriguez, *M. Materials Science and Engineering B*. **163** (2009) 190-193.
28. Biswas Kanishka, Sardar, Kripasindhu and Rao C. N R. *Applied Physics Letters*. **89** (2006) 132503 - 132503-3
29. X. M. Caia *et al.*, *Materials Science and Engineering B*. **117** (2005) 292-295.
30. B. Hu *et al.*, *Applied Surface Science* **258** (2011) 525-529.